Electronic Supplementary Material (ESI) for Physical Chemistry Chemical Physics.

Supplementary Information

Electrocatalytic N_2 Reduction Activity of Core-Shell Iron Nanoalloy Catalysts – A Density Functional Theory (DFT) Study

Arunendu Das,[†] Sandeep Das,[†] and Biswarup Pathak[*,†]

†Department of Chemistry, Indian Institute of Technology Indore, Indore 453552, India

*Email: biswarup@iiti.ac.in

Table S1. Calculated values of cohesive and formation energy, core-shell interaction energy (CSIE), average Fe-Fe and Fe-M bond length in Å and magnetic moment (μ_B/atom) for all clusters considered.

Systems	Cohesive energy (eV)	Formation energy (eV)	CSIE (eV)	Average bond length (Å)		Magnetic Moment (μ_B/atom)
				Fe-Fe in shell	Fe(shell)-M(core)	
Co@Fe	-4.25	1.20	-0.80	2.407	2.359	2.66
Ni@Fe	-4.08	1.25	-0.62	2.402	2.394	2.42
Cu@Fe	-3.74	1.33	-0.48	2.397	2.436	2.23
Fe_{65}	-4.20	1.19	-0.65	2.407	2.398	2.79

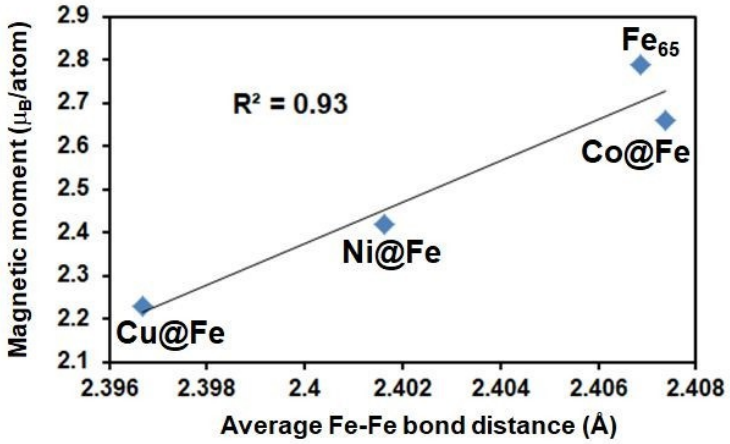

Figure S1. Magnetic moment (μ_B/atom) plotted against average Fe-Fe bond distance (Å) for all clusters considered.

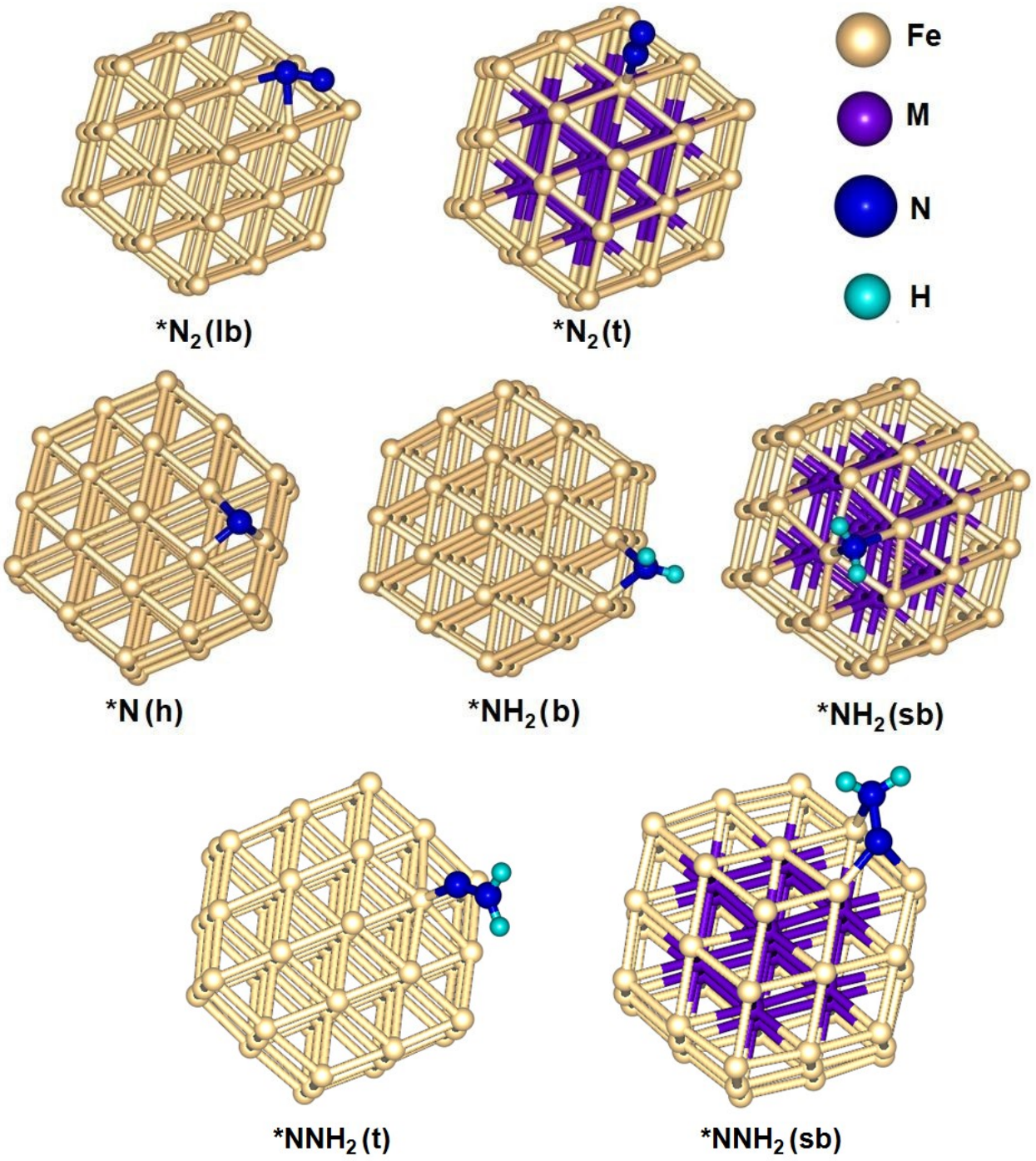

Figure S2. Possible adsorption sites (lb, t, h, b, sb) over (110) facet of Fe_{65} and M@Fe clusters for adsorbed species. Adsorbed *N_2 with side on [*N_2 (lb)] and end-on fashion [*N_2 (t)], adsorbed *N, *NH_2 and *NH_2 at hollow (h), bridge (b) and short-bridge (sb) sites, adsorbed *NNH_2 at top (t) and short-bridge (sb) sites, respectively.

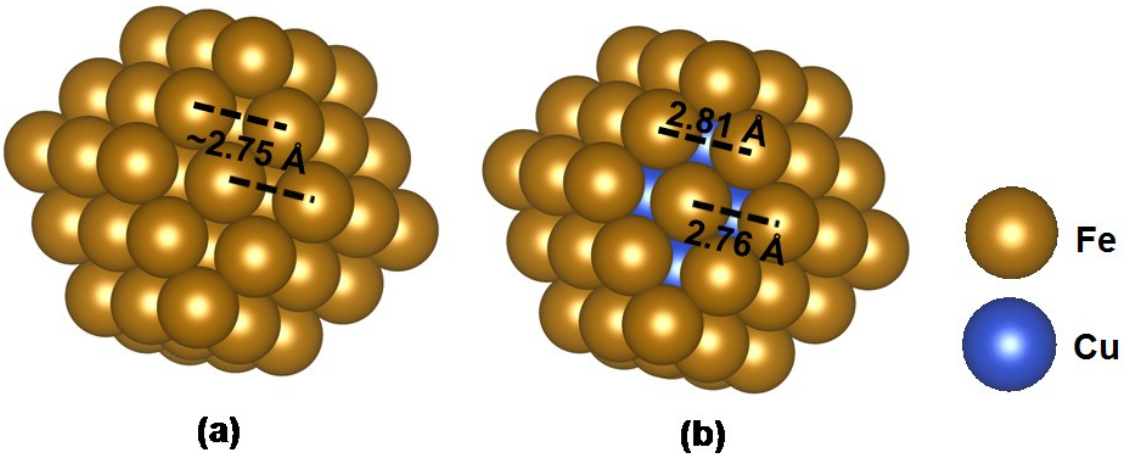

Figure S3. Bond distances at short-bridge (sb) active sites on (a) Fe_{65} NC and (b) Cu@Fe NC.

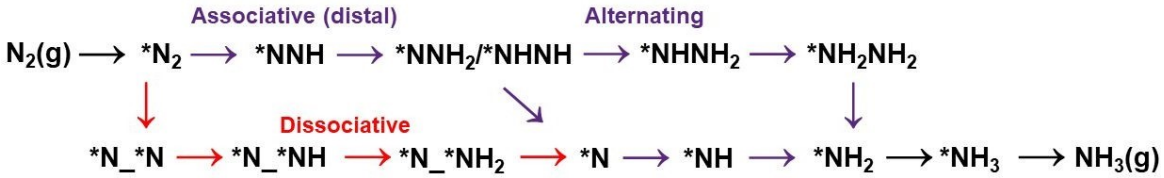

Figure S4. Possible elementary mechanisms of N_2 reduction to NH_3 include dissociative and associative(distal and alternating) mechanism.[1-3]

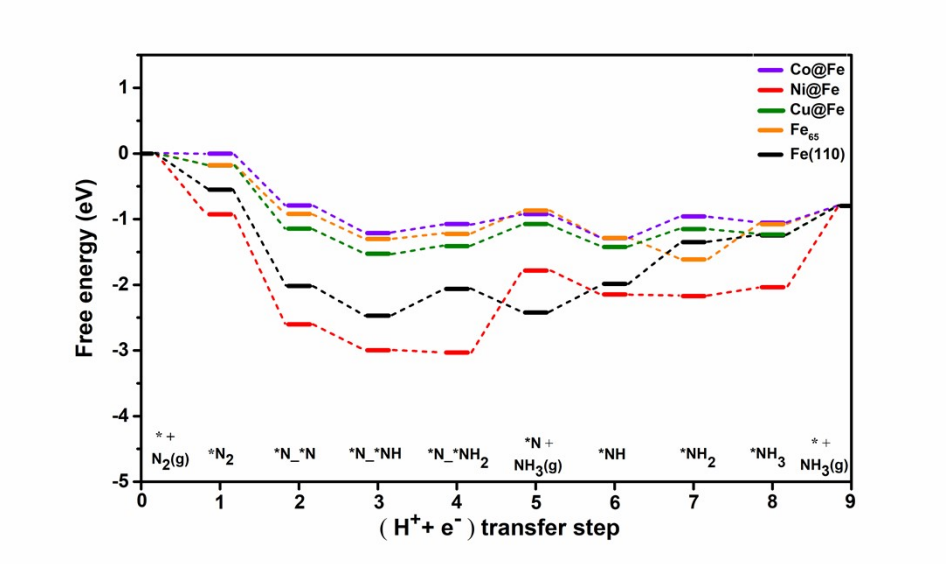

Figure S5. Reaction free energy diagram for the dissociative mechanism without applied bias (U= 0 V).[4]

Table S2. ΔG_{max} values with PDS, working potential (U_{work}) following dissociative and associative pathway for all the considered clusters and reported catalysts.[4]

Pathway	Systems	PDS	ΔG_{max} (eV)	Working potential $U_{work} = [-\Delta G_{max}/e$ in V]
Dissociative	Co@Fe	$*NH + (H^+ + e^-) \rightarrow *NH_2$	0.33	-0.33
	Ni@Fe	$*N\_*NH_2 + (H^+ + e^-) \rightarrow *N + NH_3$ (g)	1.25	-1.25
	Cu@Fe	$*N\_*NH_2 + (H^+ + e^-) \rightarrow *N + NH_3$ (g)	0.34	-0.34
	Fe_{65}	$*NH_2 + (H^+ + e^-) \rightarrow *NH_3$	0.53	-0.53
	Fe(110)[4]	$*N\_*NH_2 + (H^+ + e^-) \rightarrow *N + NH_3$ (g)	0.51	-0.51
	Fe_{85}-NC[4]	$*NH_2\_*NH_2 + (H^+ + e^-) \rightarrow *NH_2 + NH_3$	0.45	-0.45
Distal Associative	Co@Fe	$*NH + (H^+ + e^-) \rightarrow *NH_2$	0.33	-0.33
	Ni@Fe	$*N_2 + (H^+ + e^-) \rightarrow *N_2H$	0.94	-0.94
	Cu@Fe	$*NH + (H^+ + e^-) \rightarrow *NH_2$	0.27	-0.27
	Fe_{65}	$*NNH + (H^+ + e^-) \rightarrow *NNH_2$	1.06	-1.06
	Fe(110)[4]	$*NH + (H^+ + e^-) \rightarrow *NH_2$	0.50	-0.50
	Fe_{85}-NC[4]	$*N_2 + (H^+ + e^-) \rightarrow *N_2H$	0.42	-0.42

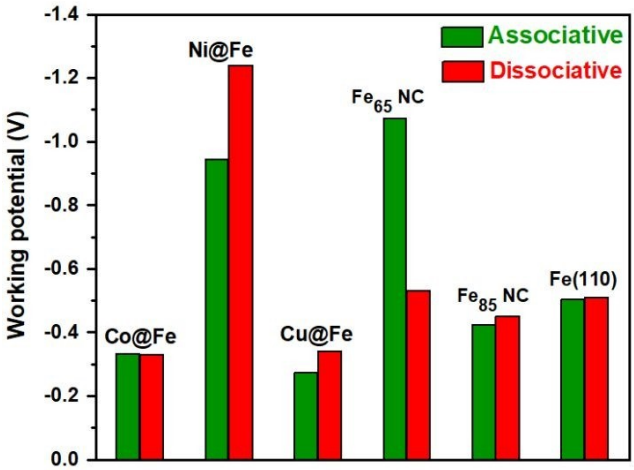

Figure S6. Working potential (V) for M@Fe clusters, reported $Fe_{85}NC$ and pristine Fe(110) following dissociative and associative pathway.[4]

Table S3. Calculation details associated with the reaction free energy change (ΔG) of $*N_2 \rightarrow$ *NNH for M@Fe clusters.

Systems	$\Delta G_{*N2 \rightarrow *NNH}$ (eV)
Co@Fe	0.22
Ni@Fe	0.95
Cu@Fe	0.14

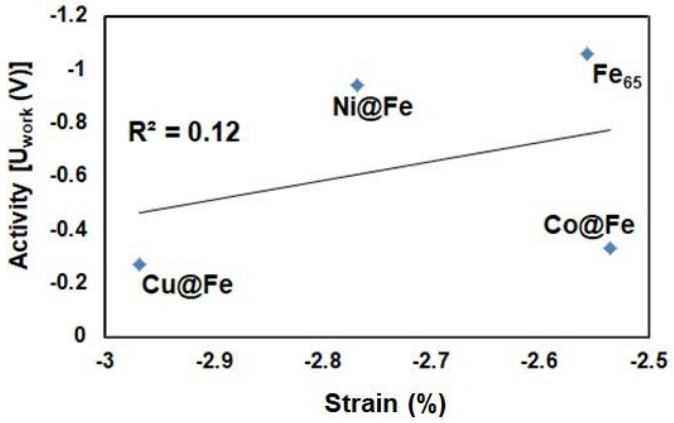

Figure S7. Activity [U_{work} in V] plotted against compressive strain (%) for all the considered clusters. The shortest Fe-Fe bond distance in reported pristine Fe(110) is 2.47Å.[4]

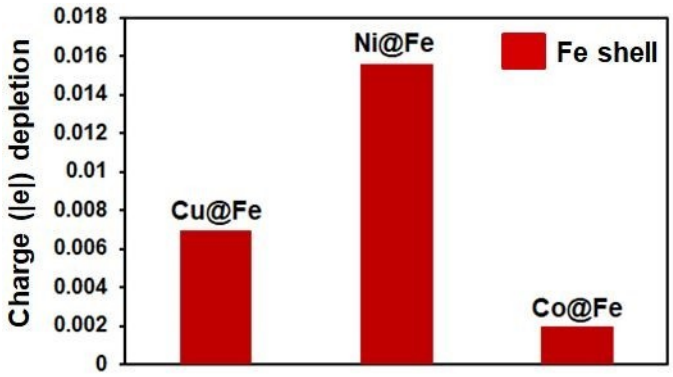

Figure S8. Charge depletion on Fe shell atoms obtained from Bader analysis for M@Fe clusters.

Table S4. Calculated values of average d-band center of outer shell Fe atoms for all the considered cluster.[5]

Systems	d-band center (ε_{Fe})
Co@Fe	-1.29
Ni@Fe	-1.26
Cu@Fe	-1.09
Fe_{65}	-1.43

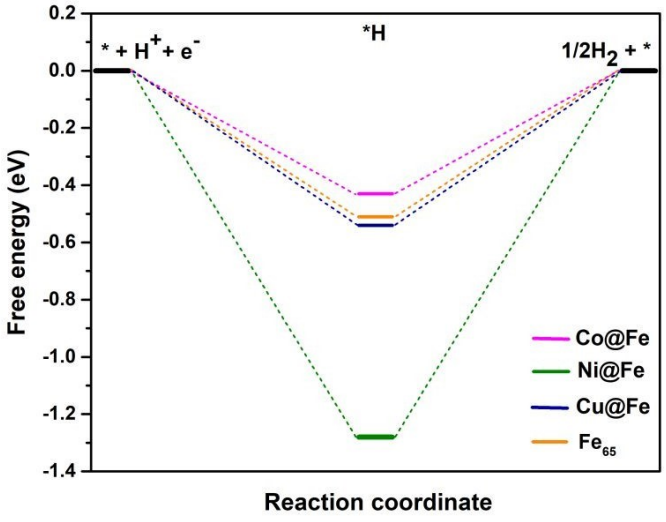

Figure S9. HER free energy diagram for all the considered catalysts.[6,7]

Table S5. Calculation details associated with the reaction free energy change (ΔG) of $*N_2$ and *H, exchange current density (i_0), NRR/HER overpotential for M@Fe and Fe_{65} NCs.

Systems	ΔG_{*N2} (eV)	ΔG_{*H} (eV)	Exchange current density (i_0)	Log (i_0/Acm^{-2})	Overpotential (η in V)	
					NRR	HER
Co@Fe	-0.03	-0.43	5.07×10^{-08}	-7.29	0.20	0.43
Ni@Fe	-0.92	-1.28	1.92×10^{-22}	-21.71	0.81	1.28
Cu@Fe	-0.18	-0.54	6.90×10^{-10}	-9.16	0.14	0.54
Fe_{65}	-0.14	-0.51	2.22×10^{-09}	-8.65	0.40	0.51

According to the computational hydrogen electrode (CHE) model, the η value can be determined by the equation as follows,

$$\eta_{NRR} = U_{eq} - U_{work} \text{ (V)}$$

$$= -0.13 - U_{work} \text{ (V)}$$

where, U_{eq} is the equilibrium potential of NRR (−0.13 V for $N_2 + 6H^+ + 6e^- \rightarrow 2NH_3$)

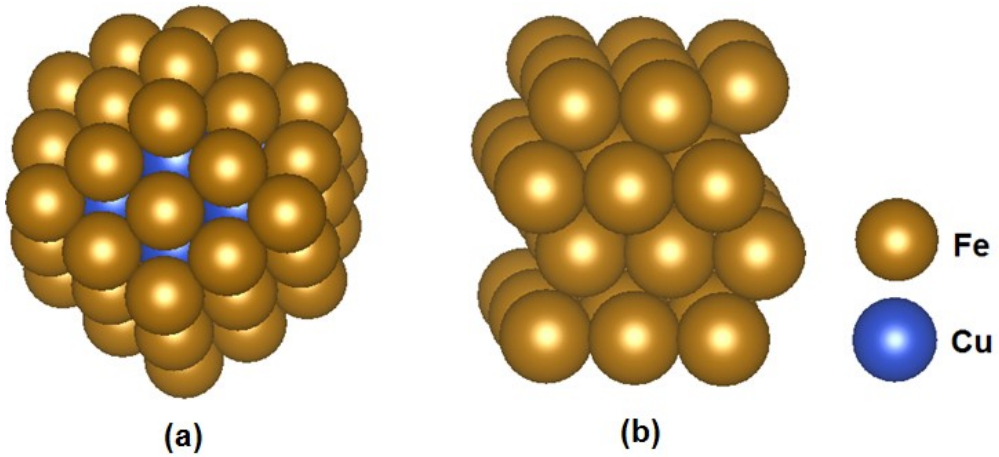

Figure S10. (a) Cu@Fe NC and (b) reported Fe(110) surface in defected form.[4]

References

(1) G. Ertl, *Catal. Rev.*, 1980, **21**, 201–223.

(2) L. C. Seefeldt, B. M. Hoffman and D. R. Dean, *Annu. Rev. Biochem.*, 2009, **78**, 701–722.

(3) M. J. Dilworth and R. R. Eady, *Biochem. J.*, 1991, **277**, 465–468.

(4) A. Das, A. S. Nair, S. C. Mandal and B. Pathak, *ACS Appl. Nano Mater.*, 2021, **4**, 7758−7770.

(5) J. K. Nørskov, F. Abild-Pedersena, F. Studta and T. Bligaard, *Proc. Natl. Acad. Sci.*, 2011, **108**, 937–943.

(6) Y. Abghoui and E. Skulason, *J. Phys. Chem. C*, 2017, **121**, 6141−6151.

(7) A. S. Nair, R. Ahuja and B. Pathak, *Nanoscale Adv.*, 2020, **2**, 2410−2421.